THE PHOTODETECTOR ARRAY CAMERA & SPECTROMETER (PACS) FOR HERSCHEL

A. Poglitsch[1], C. Waelkens[2], and N. Geis[1]

[1]Max-Planck-Institut für extraterrestrische Physik, Postfach 1312, D-85741 Garching, Germany
[2]Katholieke Universiteit Leuven, Celestijnenlaan 200B, B-3001 Leuven, Belgium

Abstract

The Photodetector Array Camera and Spectrometer (PACS) is one of the three science instruments for ESA's far infrared and submillimetre observatory Herschel. It employs two Ge:Ga photoconductor arrays (stressed and unstressed) with 16×25 pixels, each, and two filled Si bolometer arrays with 16×32 and 32×64 pixels, respectively, to perform imaging line spectroscopy and imaging photometry in the $60 - 210\mu$m wavelength band. In photometry mode, it will simultaneously image two bands, $60-90$ or $90-130\mu$m and $130-210\mu$m, over a field of view of $\sim 1.75' \times 3.5'$, with full beam sampling in each band. In spectroscopy mode, it will image a field of $\sim\ 50'' \times 50''$, resolved into 5×5 pixels, with an instantaneous spectral coverage of $\sim$ 1500km/s and a spectral resolution of $\sim$ 175km/s. In both modes background-noise limited peformance is expected, with sensitivities (5σ in 1h) of ~ 3 mJy or $2 - 8 \times 10^{-18}$W/m^2, respectively.

Key words: Instruments: far infrared – Instruments: space – Instruments: photometer, integral field spectrometer – Missions: Herschel

1. Introduction

The far infrared and submillimetre satellite Herschel will open up the wavelength range $\leq 80 - 600\mu$m to photometry and spectroscopy with unprecedented sensitivity and spatial resolution, unobscured by the Earth's atmosphere.

Within the complement of three instruments selected to form the science payload, the shortest wavelength band, $60 - 210\mu$m, will be covered by the Photodetector Array Camera & Spectrometer (PACS), which will provide both photometric and spectroscopic observing modes suited to address the key scientific topics of the Herschel mission.

In this paper we describe the design of PACS which has been developed by a consortium of European research institutions with the goal to build and operate the instrument and the associated Instrument Control Centre. This design is the outcome of an iterative optimization process toward best observing efficiency regarding the key science of Herschel and toward simplicity of operation, and in the context of complementary missions like SOFIA or SIRTF.

2. Instrument Requirements

The advantage of Herschel in its core wavelength range – compared to missions like SIRTF and SOFIA or ground based facilities – is its unique combination of angular resolution and sensitivity which enables the scientific program forseen with Herschel. The key science to be addressed with Herschel requires from PACS the provision of diffraction/telescope-limited, broad-band photometric imaging, and of medium-resolution spectroscopic capabilities, at wavelengths from $\sim 60\mu$m to $> 200\mu$m. The lower wavelength limit is mainly determined by the surface quality of the Herschel telescope; at shorter wavelengths Herschel will not be able to maintain its advantage over SIRTF in terms of angular resolution.

2.1. Photometer Requirements

Photometric color diagnostics requires spectral bands with a relative bandwidth $\Delta\lambda/\lambda < 1/2$. In coordination with SPIRE, the PACS photometric bands have been defined as $60 - 90\mu$m, $90 - 130\mu$m, and $130 - 210\mu$m.

A major fraction of the Herschel observing time will go to deep and/or large scale photometric surveys. For these, mapping efficiency is of the highest priority. Mapping efficiency is determined by both, the instantaneous field of view of the instrument (number of pixles) and the sensitivity per pixel. How the two parameters enter into a measure of the mapping efficiency greatly depends on the mapped objects. A main discriminator is the confusion limit (source separation $\sim$ a few beam diameters): If confusion is reached after a reasonably short integration time, then sensitivity per detector can be traded for number of pixels. In the opposite case, the sensitivity per pixel is the more important parameter. Within the PACS bands, the confusion limit in selected fields is expected as low as a few mJy (5σ), and detector sensitivity (if a trade-off turned out necessary) has to get higher priority than number of pixels. Thus, the PACS instrument had to be designed around the largest possible detector arrays affordable without a compromise in sensitivity, i.e., with the highest possible system detective quantum efficiency and telescope background limited noise performance.

Simultaneous observation of – preferably all – photometric bands is also suggested by the need to maximize observing efficiency, and a by-product when detector tech-

Proc. Symposium *'The Promise of the Herschel Space Observatory'* 12–15 December 2000, Toledo, Spain
ESA SP-460, July 2001, eds. G.L. Pilbratt, J. Cernicharo, A.M. Heras, T. Prusti, & R. Harris

nology requires different detectors to cover the full PACS wavelength band with optimum sensitivity.

Extraction of very faint sources from the very bright telescope background has to be ensured, by a combination of instrinsic photometric stability and ways to precisely flat-field the system responsvity on as short a timescale as necessary, as well as by spatial modulation techniques (chopping/nodding, on-the-fly mapping).

2.2. Spectrometer Requirements

The key spectroscopic observations ask for the detection of weak spectral lines with medium resolution (R $\sim$ 1500). The sources to be observed may have precisely known positions or, in the case of follow-up observations to the photometric surveys, only within the absolute position error of the Herschel satellite. In any case, the intrinsic uncertainty in the satellite pointing should not compromise the measurement, neither in sensitivity nor in spatial resolution. Subtraction of the high telescope background must be accomplished.

Sensitivity is the most important parameter for optimisation; with background-limited performance the best sensitivity is obtained if the spectrometer fulfills the following conditions: The detection bandwidth must not be greater than the resolution bandwidth, which should be matched to the line width of the source, and the line flux from the source must be detected with the highest possible efficiency in terms of system transmission, spatial and spectral multiplexing.

Wavelength calibration accurate to a fraction of the resolution bandwidth must be ensured for all observations. Intensity calibration and removal of modulations in the spectral response (defringing) must be provided for.

3. Instrument Design

The instrument concept has been developed based on the requirements stated above on the one hand, and within the boundary conditions set by the satellite and the available detector technology on the other hand. Use of the thus defined "phase space" has been mainly defined by the resources which are at the disposal of the PACS consortium.

The instrument will offer two basic modes in the wavelength band $60-210\mu$m:

- Imaging dual-band photometry ($60-90$ or $90-130\mu$m and $130-210\mu$m) over a field of view of $1.75' \times 3.5'$, with full sampling of the telescope point spread function (diffraction/wavefront error limited)
- Integral-field line spectroscopy between 57 and 210 μm with a resolution of $\sim$ 175 km/s and an instantaneous coverage of $\sim$ 1500 km/s, over a field of view of $\sim 50'' \times 50''$

Both modes will allow spatially chopped observations by means of an instrument-internal chopper mirror with variable throw; this chopper also is used to alternatively switch two calibration sources into the field of view.

The focal plane sharing of the instrument channels is shown in Fig. 1.

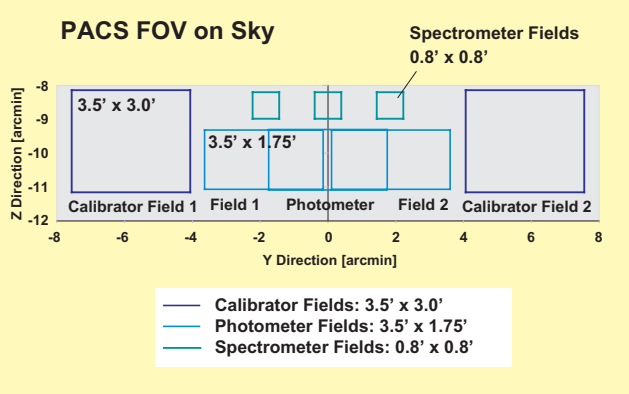

Figure 1. PACS focal plane usage. Long-wavelength and short-wavelength photometry bands cover identical fields of view. The spectrometer field of view is offset in the +z direction. Chopping is done along the y axis (left-right in this view) and also allows observation of the internal calibrators on both sides of the used area in the telescope focal plane. The chopper throw for sky observations is $\pm 1/2$ the width of the photometer field such that object and reference fields can be completely separated (photometer field 1 and 2).

The photometric bands, which can be observed simultaneously, cover the same field of view, while the field of view of the spectrometer is offset from the photometer field (Fig. 2. Since photometry and spectroscopy are mutually exclusive this has no effect on the observing efficiency.

The focal plane unit provides these capabilities through five functional units:

- common input optics with the chopper, calibration sources and a focal plane splitter
- a photometer optical train with a dichroic beam splitter and separate re-imaging optics for the short-wavelength bands ($60-90$ / $90-130\mu$m) and the long-wavelength band ($130-210\mu$m), respectively
- a spectrometer optical train with an image slicer unit for integral field spectroscopy, an anamorphic collimator, a diffraction grating in Littrow mount with associated actuator and position readout, anamorphic re-imaging optics, and a dichroic beam splitter for separation of diffraction orders
- 2 bolometer arrays with cryogenic buffers/multiplexers and a common 0.3 K sorption cooler
- 2 photoconductor arrays with attached cryogenic readout electronics (CRE)

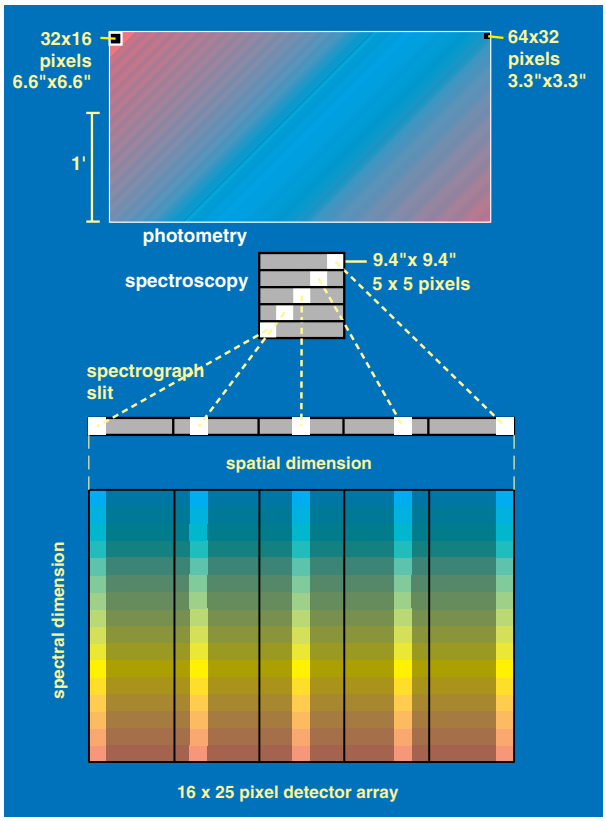

Figure 2. Focal plane footprint. A fixed mirror is used to split the focal plane into the photometry and spectroscopy channels of the instrument. In the photometry section, the two wavelength bands are simultaneously imaged with different magnification to reach full beam sampling in both bands. In the spectroscopy section, an optical image slicer re-arranges the 2-dimensional field along the entrance slit of the grating spectrograph such that, for all spatial elements in the field, spectra are observed simultaneously.

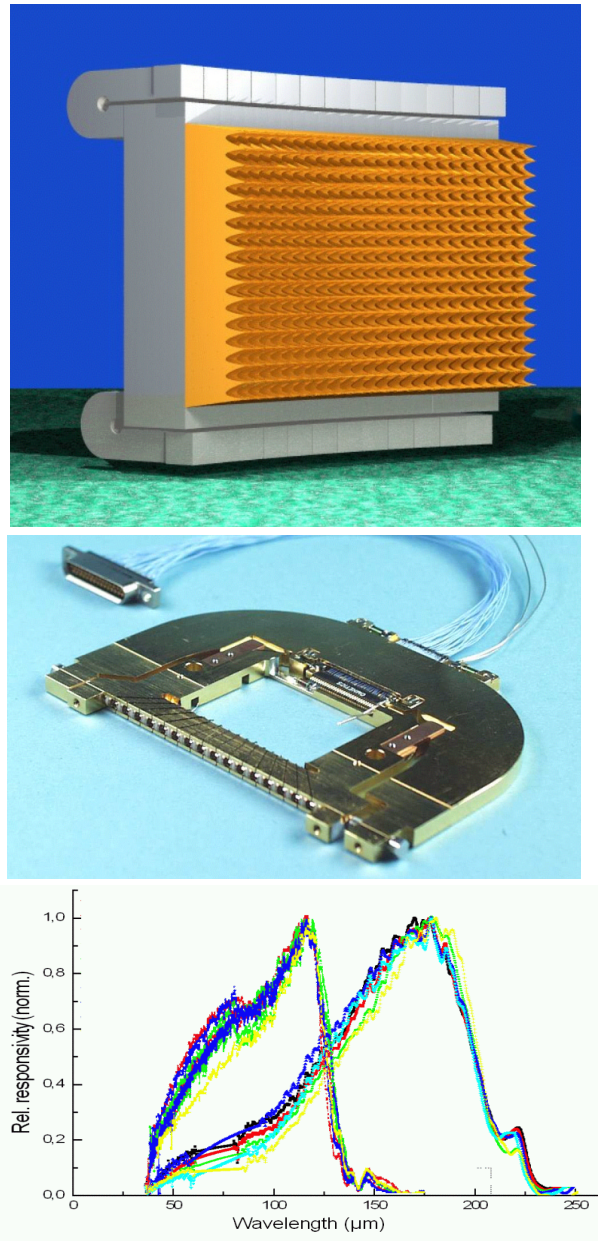

Figure 3. Top: solid model of the 25×16 *stressed Ge:Ga photoconductor array for PACS. Light cones provide for area-filling light collection onto the individual detectors. Center: One linear 16-element detector module without light cones. Stress is applied to the whole stack of Ge crystals and separating pressure "pistons" with a precision screw; the C-shaped part of the module serves as a spring clamp. Bottom: relative spectral response of stressed (long wavelength) and unstressed (short wavelength) detectors.*

3.1. Photoconductor Arrays

The 25×16 pixels Ge:Ga photoconductor arrays are a completely modular design. 25 linear modules of 16 pixels each are stacked together to form a contiguous, 2-dimensional array. For the long-wavelength band a sophisticated stressing mechanism ensures a homogeneous stress within each pixel along the entire stack of 16. The second – "unstressed" – array with improved short-wavelength responsivity is almost identical to the long-wavelength array, except for the mechanical stress on the pixels which will be reduced to about 10% of the level needed for the long-wavelength response. Details of the design of both arrays are decribed in Kraft et al. (2000).

One linear, high-stress detector module is shown in Fig. 3 (centre). The light cones in front of the actual detector block provide for area-filling light collection in the focal plane and feed the light into the individual integrating cavities around each individual, mechanically stressed pixel. The light cones also act as a very efficient means of straylight suppression because their solid angle of acceptance is matched to the re-imaging optics such that out-of-beam light is rejected. Responsivity measuremets of both stressed and unstressed modules show very homogeneous spectral response within each module (Fig. 3, bottom).

Each linear module of 16 detectors is read out by a cryogenic amplifier/multiplexer circuit in CMOS technology (Charlier 2000). The readout electronics is integrated into the detector modules. The high telescope background and the readout noise spectrum require a rapid readout (1/256 s) of each pixel which leads to a raw data rate substantially above the maximum rate allowed by the Herschel on-board data handling system. A combination of data reduction and lossless data compression (Bischof et al. 2000; Kerschbaum et al. 2000) is carried out by a dedicated Signal Processing Unit (SPU) within the PACS warm electronics.

3.2. Bolometer Arrays

The PACS bolometers will be filled arrays of square pixels which allow instantaneous beam sampling. Fig. 4 (centre) shows a cut-out of the 64×32 pixels bolometer array assembly. 4×2 monolithic sub-arrays of 16×16 pixels are tiled together to form the short-wave focal plane array. In a similar way, 2 sub-arrays of 16×16 pixels are tiled together to form the long-wave focal plane array. Fig. 4 (top) shows a development model of the 16×16 subarray with a micrograph of one pixel. The subarrays are mounted on a 0.3 K carrier which is thermally isolated from the surrounding 2 K structure. The buffer/multiplexer electronics is split in two levels; a first stage is part of the indium-bump bonded back plane of the focal plane arrays, operating at 0.3 K. Ribbon cables connect the output of the 0.3 K readout to a buffer stage running at 2 K. Details on the bolometer design are given in Agnese et al. (1999). The post-detection bandwidth (thermal/electrical) of the bolometers is ∼5 Hz; the 1/f "knee" of the bolometer/-readout system is expected to occur at a few tenths of a Hz. Because of the large number of pixels, data compression by the SPU is required. Both array assemblies are mounted on the 0.3 K cooler unit (Fig. 4 bottom) which provides uninterrupted operation for two days. This cooler is identical to the unit developed for SPIRE (Duband & Collaudin 1999).

3.3. Entrance Optics, Chopper and Calibrators

The entrance optics (see Fig. 5) fulfills the following tasks: It creates an image of the telescope secondary mirror (the entrance pupil of the telescope) on the instrument chopper; this allows spatial chopping with as little as possible modulation in the background received by the instrument. It also provides for an intermediate pupil position where the Lyot stop and the first blocking filter, common to all instrument channels, can be positioned, and it allows the chopper – through two field mirrors adjacent to the used field of view in the telescope focal surface – to switch between a (chopped) field of view on the sky and two calibration sources (see also Fig. 1).

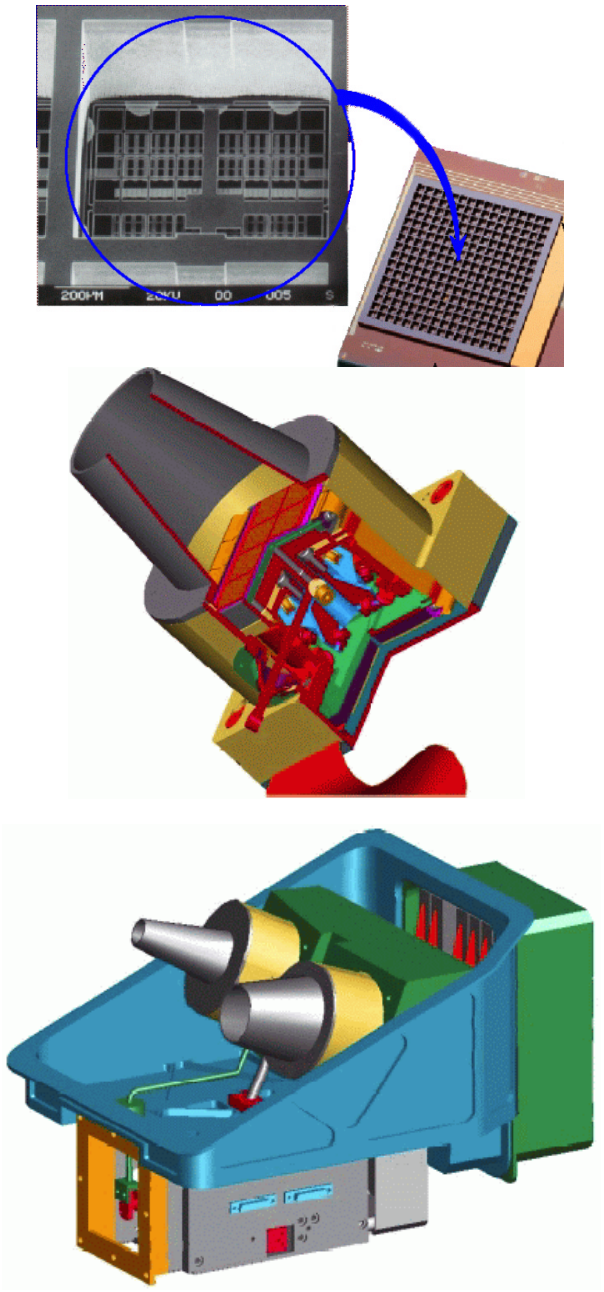

Figure 4. Top: Micrograph of one pixel of the filled bolometer array development model. The physical size of a PACS pixel will be 0.75 mm. The absorber and back-reflector grids as well as the integrated thermistor are monolithic silicon structures. Centre: solid model of the 64×32 *pixels (short-wave) bolometer array for PACS. The cutout shows the* 4×2 *subarrays of* 16×16 *pixels mounted to a 0.3 K carrier plate which is suspended from the 2 K housing. Bottom: the bolometer unit with the two array assemblies and the 0.3 K sorption cooler to which the focal plane carrier plates are thermally linked.*

The chopped image is then re-imaged onto an intermediate focus where a fixed field mirror splits off the light into the spectroscopy channel. The remaining part of the

field of view passes into the photometry channels. A "footprint" of the focal-plane splitter is shown in Fig. 2.

The calibration sources are placed at the entrance to the instrument to have the same light path for observation and internal calibration. This is essential for removing baseline ripples as best as possible, a serious task with a warm telescope and the associated high thermal background. To eliminate non-linearity or memory problems with the detector/readout system, the calibrator sources will be gray-body sources providing FIR radiation loads slightly above or below the telescope background, respectively. They also mimic the illumination of the telescope.

The chopper provides a maximum throw of $4'$ on the sky; this allows full separation of an "object" field and a "reference" field. The chopper (Lemke et al. 1999) is capable of following arbitrary waveforms with a resolution of $1''$ and delivers a duty-cycle of ∼90% at a chop frequency of 5 Hz.

3.4. Imaging Photometer

After the intermediate focus provided by the entrance optics, the light is split into the long-wavelength and short-wavelength channels by a dichroic beamsplitter with a transition wavelength of 130μm and re-imaged with different magnification onto the respective bolometer array.

The 32×16 or 64×32 pixels in each array are used to image a field of view of $3.5' \times 1.75'$ in both channels, providing full beam sampling at 90μm and 180μm, respectively. The long-wavelength band ($130 - 210\mu$m) can be combined with either one of the two bands of the short-wavelength channel, $60 - 90\mu$m or $90 - 130\mu$m. The two short-wavelength bands are selected by two filters with an exchange mechanism. All filters are implemented as multi-mesh interference filters and provided by QMW[1].

The re-imaging optics also creates exit pupils at appropriate distances from the bolometer arrays to allow efficient baffling with the bolometer assemblies.

3.5. The Integral-Field Spectrometer

The spectrometer (see Fig. 5) covers the wavelength range from 57μm to 210μm. It provides a resolving power of $1000 - 2000$ (Δv = 150 − 300km/s) with an instantaneous coverage of ∼ 1500km/s and simultaneous imaging of a ∼ $50'' \times 50''$ field of view, resolved into 5×5 pixels. An image slicer employing reflective optics is used to re-arrange the 2-dimensional field of view along a 1×25 pixels entrance slit for a grating spectrometer, as schematically shown in Fig. 2.

The integral-field concept has been selected because simultaneous spectral and spatial multiplexing allows the most efficient detection of weak individual spectral lines with sufficient baseline coverage and high tolerance to pointing errors without compromising spatial resolution, as well as for spectral line mapping of extended sources regardless of their intrinsic velocity structure.

The Littrow-mounted grating with a length of ∼ 30cm is operated in 1st, 2nd or 3rd order, respectively, to cover the full wavelength range. The 1st order covers the range $105 - 210\mu$m, the 2nd order $72 - 105\mu$m, and the 3rd order $57 - 72\mu$m. Anamorphic collimating optics expands the beam to an elliptical cross section to illuminate the grating over a length required to reach the desired spectral resolution. The grating is actuated by a cryogenic motor (Renotte et al. 1999) with a resolution of a few arcsec which allows spectral scanning/stepping for improved spectral flatfielding and for coverage of extended wavelength ranges.

The light from the 1st diffraction order vs. light from the other two orders is separated by a dichroic beam splitter and passed on into two optical trains feeding the respective detector array (stressed/unstressed) for the wavelength ranges $105 - 210\mu$m and $57 - 105\mu$m. Anamorphic re-imaging optics is employed to independently match the spatial and spectral resolution of the system to the square pixels of the detector arrays. The filter exchange mechanism in the short-wavelength path selects the 2nd or 3rd grating order.

4. Observing Modes

The observing modes supported by PACS are combinations of *instrument modes* and *satellite pointing modes*. All satellite pointing modes – stare, raster, and line scan (with or without nodding) – are foreseen to be used for PACS observations. The following section describes the PACS instrument modes.

4.1. Dual-band Photometry

In this mode, both bolometer arrays are operating, providing full spatial sampling in each band. The long-wave array images the $130 - 210\mu$m band while the short-wave array images either the $60 - 90$ or the $90 - 130\mu$m band. The respective sub-band is selected by a filter. This mode is the standard mode for PACS as prime instrument. Observing parameters are the chopper mode (off/on; waveform, throw), pointing parameters (stare/raster/scan;nod), and the integration time per pointing.

4.2. Single-band Photometry

In this mode, only one bolometer array is operating such that either the long-wave array images the $130 - 210\mu$m band or short-wave array images the $60 - 90$ or the $90 - 130\mu$m band. This mode serves as a test mode for PACS as prime instrument, but it is also foreseen as standard mode for PACS/SPIRE parallel observations. Observing param-

[1] P.A.R. Ade, Department of Physics, Queen Mary and Westfield College, London

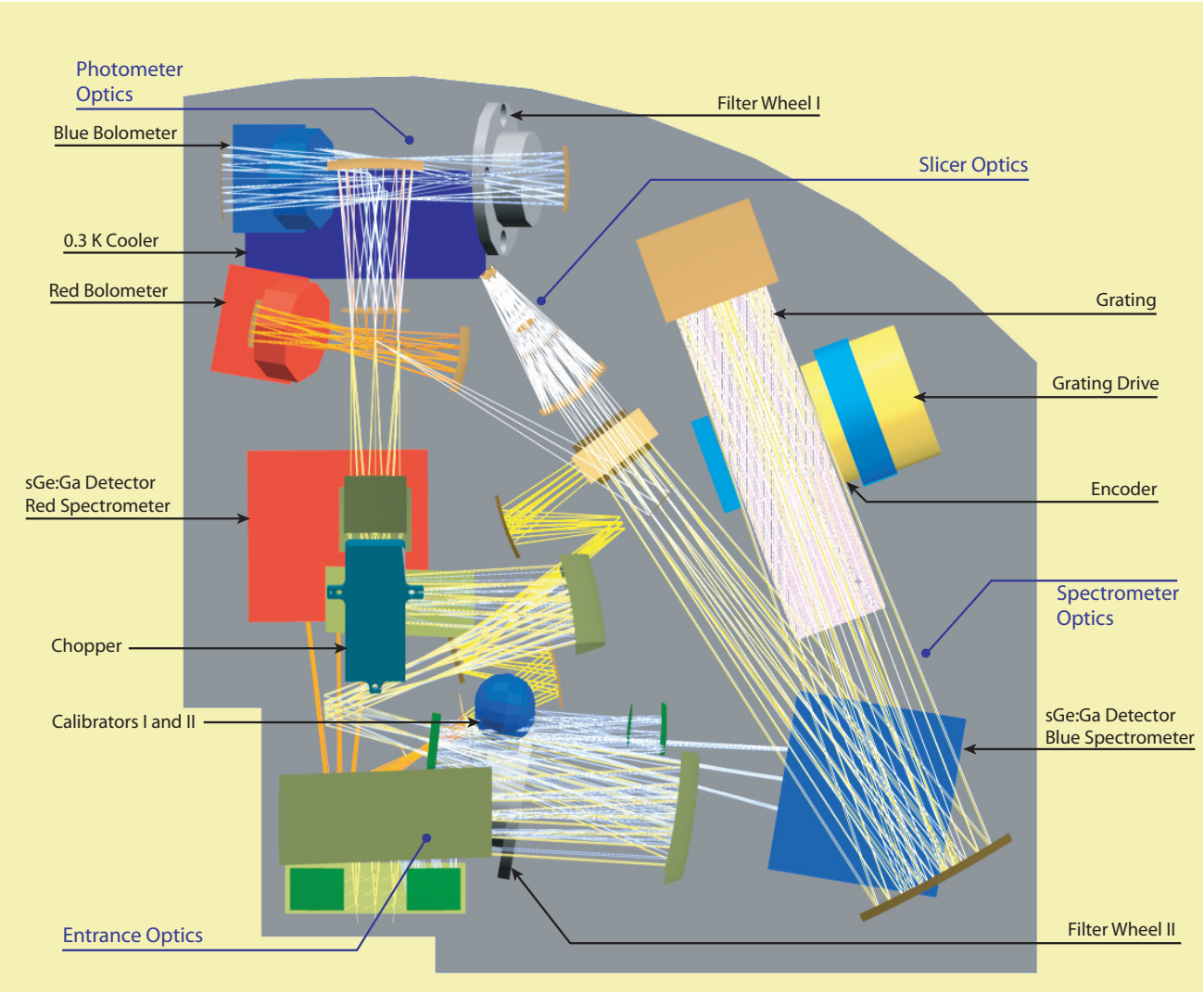

Figure 5. PACS Focal Plane Unit: After the common entrance optics with calibrators and the chopper, the field is split into the spectrometer train and and the photometer trains with a dichroic beam splitter and separate re-imaging optics for the two bolometer arrays. In the spectrometer train, the image slicer converts the square field into an effective long slit for the Littrow-mounted grating spectrograph. The dispersed light is distributed to the two photoconductor arrays by a dichroic beam splitter which acts as order sorter for the grating.

eters are the chopper mode (off/on; waveform, throw), pointing parameters (stare/raster/scan;nod), and the integration time per pointing.

4.3. Line Spectroscopy

In this mode, one or two photoconductor arrays are operating for observations of individual lines. The long-wave array will observe in the $105-210\mu$m band while the short-wave array observes in the $57-72$ or $72-105\mu$m band. The wavelength in the primary band automatically determines the wavelength in secondary band; therefore, for most practical purposes, one can assume that only one line can be observed at a time, and only one array needs to be read out. This will help to reduce the integrated data rate. Observing parameters are the scan width (default 0), the chopper mode (off/on; waveform, throw), pointing parameters (stare/raster/scan;nod), and the integration time per pointing.

4.4. Range Spectroscopy

In this mode, both photoconductor arrays are operating for effective observations of extended wavelength ranges. Such observations can be continuous scans with full spectral resolution or steps for a coarser sampling of, e.g., SEDs. The long-wave array will observe in the $105-210\mu$m band while the short-wave array observes in the $57-72$ or $72-105\mu$m band. Observing parameters are the start- and end wavelength, the resolution mode, the chop-

per mode (off/on; waveform, throw), pointing parameters (stare/raster/scan;nod), and the integration time per pointing.

5. System Performance

Based on the present knowledge of the components of PACS and of the Herschel satellite, the performance of the entire system can be estimated in terms of what the observer is concerned with, i.e., an assessment of what kind of observations will be feasible with Herschel/PACS, and how much observing time they will require.

The system sensitivity of the instrument at the telescope depends mainly on the optical efficiency, i.e. the fraction of light from an astronomical source arriving at the telescope that actually reaches the detector, and on the thermal background radiation from the telescope or from within the instrument as long as the fluctuations of the background constitute the dominant noise source. As will be shown below, background-noise limited performance can be reached in both spectroscopy and photometry modes with state-of-the-art detectors.

5.1. Optical Efficiency

The system optical efficiency has been modeled to the following level of detail:

- *Telescope efficiency:* The fraction of the power of a point source in the central peak of the point spread function is modeled in terms of absorption/obstruction, diffraction, and geometrical wave front errors (6μm r.m.s.), which have been assumed to occur as spherical aberration.
- *Chopper:* Errors/jitter in the chopper throw and the duty cycle ($> 80\%$) are considered.
- *Mirrors and filters:* scatter/absorption losses – excluding diffraction – on each reflection by a mirror (1%) and efficiencies of filters/dichroics (40% in total) are taken into account.
- *Diffraction:* An end-to-end diffraction analysis with the physical optics package GLAD 4.5 has been carried out for the spectrometer, where the image slicer is the most critical element of the PACS optics (Poglitsch et al. 1999), and a simplified analysis for the less critical photometer as well as the effect of diffraction/vignetting by the entrance field stop and Lyot stop have been included.
- *Grating efficiency:* The grating has been analysed and optimised with a full electromagnetic code (Poglitsch et al. 1999); a mean efficiency of 65% is achieved.

5.2. Detectors

The projected (dark) detector NEP of the Ge:Ga photoconductors is $\leq 5 \times 10^{-18}$ W Hz$^{-1/2}$, a value which will ensure background-limited performance and which has already been reached with similar designs in a balloon-borne experiment (Hiromoto et al. 1989). Detective quantum efficiencies of $\sim 30\%$ are feasible with careful cavity design (Stacey et al. 1992). Our first measurements of the fully stressed PACS modules with laboratory readout electronics even indicate a quantum efficiency near 40%.

For the bolometers, the calculated background noise from the telescope is $\sim 3 \times 10^{-16}$ W Hz$^{-1/2}$. To ensure background-limited performance we require an electrical NEP of $\leq 10^{-16}$ W Hz$^{-1/2}$ which has been demonstrated with a prototype 16×16 bolometer subarray of a design which is very similar to the final design for PACS. The calculated absorption efficiency (equivalent to the detective quantum efficiency) is $>80\%$.

5.3. Image Quality and Beam Sampling

The photometer optics delivers diffraction-limited image quality (Strehl ratio $\geq$95%). We therefore assume that the instrument optics will only contribute in a negilible way to the dilution of the central peak of the telescope PSF.

The concept of approximately full beam sampling with our (filled) array will distribute the flux of a point source over several pixels. An equivalent dilution applies to the background received by the pixel. To recover the total flux (in the central peak of the PSF) several pixels have to be co-added. For the calculation of the system sensitivity this is taken into account through a pixel efficiency factor, which is defined as the fraction of the pixel area to the PSF area.

The spectrometer, and in particular its image slicer, is used over a large wavelength range. The (spatial) pixel scale is a compromise between resolution at short wavelengths and observing efficiency (mapped area) at long wavelengths. Full spatial sampling will require a fine raster with the satellite, for spectral line maps with full spatial resolution. For the sensitivity calculation this is neglected as the line flux will always be collected with the filled detector array. Therefore, for the plain detection of a line source, one pointing is sufficient. Fully resolved maps will require between 2 and 8 raster pointings, between the long and short wavelength end of the spectrometer range, with correspondingly longer integration time.

The spectral sampling also varies within each grating order; detection to the instantaneous resolution as given by the convolution of the diffraction-limited resolution with the pixel function is the default for the sensitivity estimates.

5.4. System Sensitivity

For the calculation of the system sensitivity we have included our present best knowledge of all components in the detection path as described above. The following tables summarise the pertinent performance data for photometry and spectroscopy.

Pixel size	$3.3''$	$6.6''$
FOV	$3.5' \times 1.75'$	$3.5' \times 1.75'$
Wavelength range	$60 - 90/90 - 130\mu$m	$130 - 210\mu$m
Point source detection limit (5 σ, 1 hour)	3.1/3.0 (2.2/2.1)* mJy	3.2 (2.3)* mJy

*) with on-array chopping

Table 1. PACS Photometer Mode Specifications

Pixel size		$9.4''$
FOV (5 ×5 pixel)		$47'' \times 47''$
Wavelength range		57μm–210μm
Resolution ($c\Delta\lambda/\lambda$)		100 – 250 km/s *
Instantaneous spectral coverage		1300 – 3000 km/s *
Point source detection limit (5 σ, 1 hour)	$\lambda = 60\mu$m	$7.8(5.5)^{**} \times 10^{-18}$W/m^2
	$\lambda = 90\mu$m	$4.0(2.8)^{**} \times 10^{-18}$W/m^2
	$\lambda = 130\mu$m	$2.8(2.0)^{**} \times 10^{-18}$W/m^2
	$\lambda = 180\mu$m	$2.5(1.8)^{**} \times 10^{-18}$W/m^2

*) varies with wavelength
**) with on-array chopping

Table 2. PACS Spectrometer Mode Specifications

5.5. Comparison with Other Missions

In Table 3 average numbers for the sensitivity of PACS over its wavelength range are compared with those of similar, existing or planned instruments on other spaceborne or airborne platforms.

Mode	Herschel-PACS	SOFIA	SIRTF
Photometry	3 (2)* mJy	50 mJy	8–55 mJy**
Spectroscopy	4×10^{-18}W/m^2	2.5×10^{-17}W/m^2	—

*) with on-array chopping
**) confusion limited

Table 3. Sensitivity of Herschel-PACS (point source detection, 5 σ, 1 hour) compared to present and planned platforms.

Even if we neglect the advantage of Herschel in terms of angular resolution, it is obvious that for point source detection PACS will have better limiting sensitivity than any other mission in the FIR in the foreseeable future. In its medium-resolution line spectroscopy mode it will be unrivaled. For point source photometry, SIRTF will be superiour in terms of raw sensitivity, but fall short for deeper surveys due to confusion. For extended sources where the angular resolution of Herschel is not required, SIRTF with its cryogenic telescope will clearly be the instrument of choice and an ideal complement to Herschel.

Acknowledgements

This paper represents work carried out by the PACS consortium which consists at this time of the following institutes: Max-Planck-Intitut für extraterrestrische Physik (MPE; D), Max-Planck-Institut für Astronomie (MPIA; D), Universitätssternwarte Jena (D), Katholieke Universiteit Leuven (KUL; B), Interuniversity MicroElectronics Centre (IMEC; B), Centre Spatial de Liège (CSL; B), Commissariat a l'Energie Atomique (CEA-SAp; F), Observatoire Astronomique de Marseille-Provence (OAMP; F), Universität Wien + Technische Universität Wien (A), Instituto de Astrofisica de Canarias (IAC; E), Osservatorio Astrofisico di Arcetri (OAA; I), Istituto di Fisica dello Spazio Interplanetario (IFSI; I), Universita di Padova (I).

References

Agnese, P., Buzzi, C., Rey, P., Rodriguez, L., Tissot, J.-L. 1999, Infrared Technology and Applications XXV, B. Andresen and M. Scholl, eds., Proc. SPIE 3698, 284

Bischof H., Belbachir, A.N., Hoenigmann D., Kerschbaum, F. 2000, UV, Optical, and IR Space Telescopes and Instruments, J. Breckinridge and P. Jakobsen, eds., Proc. SPIE 4013, 244

Charlier O. 2000, UV, Optical, and IR Space Telescopes and Instruments, J. Breckinridge and P. Jakobsen, eds., Proc. SPIE 4013, 325

Duband L., Collaudin, B. 1999, Cryogenics, v. 39, iss. 8, 659

Kerschbaum F., Bischof H., Belbachir, A.N., Lebzelter T., Hoenigmann D. 2000, UV, Optical, and IR Space Telescopes and Instruments, J. Breckinridge and P. Jakobsen, eds., Proc. SPIE 4013, 253

Kraft S., Frenzl O., Charlier, O., Cronje, T., Katterloher R., Rosenthal D., Grözinger U., Beeman J. 2000, UV, Optical, and IR Space Telescopes and Instruments, J. Breckinridge and P. Jakobsen, eds., Proc. SPIE 4013, 233

Hiromoto N., Itabe T., Aruga T., Okuda H., Matsuhara H., Shibai H., Nakagawa T., and Saito T. 1989, IR Phys. 29, 255

Lemke D., Grözinger U., Krause O., Rohloff R., Haberland R. 1999, Infrared Spaceborne Remote Sensing VII, M. Scholl and B. Andresen, eds., Proc. SPIE 3759, 205

Poglitsch A., Waelkens C., Geis N. 1999, Infrared Spaceborne Remote Sensing VII, M. Scholl and B. Andresen, eds., Proc. SPIE 3759, 221

Renotte E., Gillis J., Jamar C., Laport P., Salée T., Crehay S. 1999, Infrared Spaceborne Remote Sensing VII, M. Scholl and B. Andresen, eds., Proc. SPIE 3759, 189

Stacey G.J., Beeman J.W., Haller E.E., Geis N., Poglitsch A., Rumitz M. 1992, Int J. IR & Millimeter Waves 13, 1689